Expected production of new exotic α emitters ^{108}Xe and ^{112}Ba in complete fusion reactions

Sh. A. Kalandarov,[1,2] G. G. Adamian,[1] N. V. Antonenko,[1,3] and J. P. Wieleczko[4]
[1]*Joint Institute for Nuclear Research, 141980 Dubna, Russia*
[2]*Institute of Nuclear Physics, 702132 Tashkent, Uzbekistan*
[3]*Mathematical Physics Department, Tomsk Polytechnic University, 634050 Tomsk, Russia*
[4]*GANIL, CEA et IN2P3-CNRS, B.P. 55027, F-14076, Caen Cedex, France*
(Received 9 March 2016; published 11 May 2016)

The production cross sections of neutron-deficient isotopes $^{108–110}$Xe and $^{112–114}$Ba in the complete fusion reactions ^{58,56}Ni + ^{54}Fe and ^{58,56}Ni + ^{58}Ni with stable and radioactive beams are studied with the dinuclear system model. The calculated results are compared with the available experimental data. The optimal beam energies and corresponding maximum production cross sections of new isotopes ^{108}Xe and ^{112}Ba are predicted.

DOI: 10.1103/PhysRevC.93.054607

I. INTRODUCTION

α decay is a useful tool to investigate the low-energy structure of neutron-deficient nuclides near magic shell closures [1]. Additional interest in the α-decay rates of nuclei around ^{100}Sn [2] is caused by the study of astrophysical processes, for which this region has been cited as the end of the rapid proton capture process due to the Sn-Sb-Te cycle [3]. The α emitters ^{107,108}Te and ^{106}Te, ^{110}Xe have been produced in the reactions ^{16}O + ^{96}Ru and ^{58}Ni + ^{58}Ni, respectively [4,5]. The nucleus ^{106}Te remained for a long time the lightest known α emitter leading to the daughter nucleus ^{102}Sn. Later on the ^{50}Cr(^{58}Ni ,3n) reaction was employed to produce the ^{105}Te nucleus, which is the fastest α emitter known so far with half-life $T_{1/2} = 0.70$ μs [6].

The production of ^{109}Xe nucleus in the fusion-evaporation reaction ^{54}Fe(^{58}Ni ,3n)^{109}Xe at beam energies 220–225 MeV and the discovery of the superallowed α-decay chain ^{109}Xe $\rightarrow$ ^{105}Te $\rightarrow$ ^{101}Sn have given new motivation to search for new emitters in this region of nuclides [7]. Further studies of the superallowed α-decay chain resulted in the observation of low-lying states in ^{101}Sn, the one-neutron system outside the doubly magic nucleus ^{100}Sn [8].

The neutron-deficient nucleus ^{114}Ba has been produced in the ^{58}Ni(^{58}Ni ,2n) reaction. The α decay of ^{114}Ba occurs with $E_\alpha = 3410$ keV energy and its half-life is 430 ms. The synthesis of the more neutron-deficient barium isotope ^{112}Ba in complete fusion reactions is interesting for two reasons [9–11]. The first one is the possibility of the observation and discovery of the superallowed α-decay chain ^{112}Ba $\rightarrow$ ^{108}Xe $\rightarrow$ ^{104}Te $\rightarrow$ ^{100}Sn which connects ^{112}Ba with the doubly magic nucleus ^{100}Sn. The second one is the possible discovery of ^{12}C cluster radioactivity [12–15] of ^{112}Ba leading again to the ^{100}Sn daughter nucleus. Note that experiments searching for the superallowed decay chain ^{112}Ba $\rightarrow$ ^{108}Xe $\rightarrow$ ^{104}Te $\rightarrow$ ^{100}Sn are planned at Argonne National Laboratory (ANL, USA), the Japan Atomic Energy Agency (JAEA, Japan), and the Grand Accéléérateur National d'Ions Lourds (GANIL, France).

In the present work, the production cross sections of isotopes $^{108–110}$Xe and $^{112–114}$Ba in the fusion reactions ^{58,56}Ni + ^{54}Fe and ^{58,56}Ni + ^{58}Ni with stable and radioactive beams are predicted. The possibility of using neutron-deficient radioactive ion beams—for example, a beam of ^{56}Ni—in the complete fusion reactions gives us a good opportunity to discover new neutron-deficient isotopes and study their decay properties. This is an interesting possibility to reach the proton drip line. Some models (for example, the mass model of Ref. [16]) predict that the neutron-deficient nuclei ^{108}Xe and ^{112}Ba are beyond the proton drip line.

Our calculations are based on the dinuclear system (DNS) model [17,18] which describes well the experimental production cross sections of individual isotopes formed in very weak decay channels [19–23]. Within the DNS model [17,18], an evolution of the system occurs in the collective coordinates of charge and mass asymmetries and relative distance R. According to the model, there are nucleon drift and nucleon diffusion between the DNS nuclei which lead to the formation of excited compound nucleus (CN) and different DNS configurations with probabilities depending on the potential energy surface and temperature of the system. The decay of excited CN and DNS configurations is described in a unique way, which allows us to describe both light particle evaporation and complex fragment emission in the same way [24]. The main ingredient of our description is the sophisticated potential energy depending on the charge (mass) asymmetry and angular momentum.

The DNS model is briefly described in Sec. II. The results of calculations for the reactions ^{56,58}Ni + ^{54}Fe and ^{56,58}Ni + ^{58}Ni are presented in Sec. III. The conclusions are given in Sec. IV.

II. MODEL

The cross section of a residual nucleus with certain mass number A and charge number Z is given as

$$\sigma_{Z,A}(E_{\mathrm{c.m.}}) = \sum_{J=0}^{J_{\max}} \sigma_{Z,A}(E_{\mathrm{c.m.}}, J) = \sum_{J=0}^{J_{\max}} \sigma_{\mathrm{cap}}(E_{\mathrm{c.m.}}, J) W^{\mathrm{sur}}_{Z,A}(E_{\mathrm{c.m.}}, J), \quad (1)$$

where σ_{cap} is the partial capture cross section which defines the transition of the colliding nuclei over the Coulomb barrier and the formation of the initial DNS when the kinetic energy $E_{\mathrm{c.m.}}$ and angular momentum J of the relative motion are

transformed into the excitation energy and angular momentum of the DNS. The probability of the production of a specific residual nucleus (Z, A) from the excited entrance channel DNS in a distinct decay channel is described by $W^{\rm sur}_{Z,A}(E_{\rm c.m.}, J)$. To calculate $W^{\rm sur}_{Z,A}(E_{\rm c.m.}, J)$, one has to find the formation-emission probability $W_{Z_1,A_1}(E_{\rm c.m.}, J)$ of a specific light particle or cluster (Z_1, A_1) from the excited system. Here, we consider the decay of the excited nuclear system as a sequential light particle ($Z_1 < 2$) evaporation, which includes neutrons, protons, deutrons, and tritons, and complex clusters ($Z_1 \geqslant 2$).

The DNS formation is described by the partial capture cross section $\sigma_{\rm cap}(E_{\rm c.m.}, J)$:

$$\sigma_{\rm cap}(E_{\rm c.m.}, J) = \pi \lambda\!\!\!^{-2}(2J+1)P_{\rm cap}(E_{\rm c.m.}, J), \qquad (2)$$

where $\lambda\!\!\!^{-2} = \hbar^2/(2\mu E_{\rm c.m.})$ is the reduced de Broglie wavelength and μ the reduced mass in the entrance channel. The transition probability is calculated with the Hill-Wheeler formula: $P_{\rm cap}(E_{\rm c.m.}, J) = \{1 + \exp[2\pi(V(R_b, J) - E_{\rm c.m.})/\hbar\omega(J)]\}^{-1}$, where the effective nucleus-nucleus potential V is approximated near the Coulomb barrier at $R = R_b$ by the inverted harmonic-oscillator potential with barrier height $V(R_b, J)$ and frequency $\omega(J)$ [20]. The maximum value of the angular momentum $J_{\rm max}$ is limited either by the kinematic angular momentum $J^{\rm kin}_{\rm max} = [2\mu(E_{\rm c.m.} - V(R_b,0))]^{1/2}R_b$ or by the critical angular momentum J_{cr}, depending on which one is smaller: $J_{\rm max} = \min\{J^{\rm kin}_{\rm max}, J_{cr}\}$.

After the system is captured in a pocket of the nucleus-nucleus potential at $R = R_m$, the relative kinetic energy is transferred into potential and excitation energy. The DNS develops in time by diffusion in the mass and charge asymmetry coordinates leading to the formation of the CN and different DNS configurations. After complete fusion, the excited CN decays by various channels including the formation a DNS and its decay.

The emission probability $W_{Z_1,A_1}(E_{\rm c.m.}, J)$ of a light particle or cluster (Z_1, A_1) is calculated as the product of the CN or DNS formation probability P_{Z_1,A_1} and the CN or DNS decay probability $P^R_{Z_1,A_1}$:

$$W_{Z_1,A_1}(E_{\rm c.m.}, J) = \frac{P_{Z_1,A_1}P^R_{Z_1,A_1}}{\sum_{Z'_1,A'_1} P_{Z'_1,A'_1}P^R_{Z'_1,A'_1}}, \qquad (3)$$

where the indexes Z'_1 and A'_1 go over all possible channels from the neutron evaporation to the symmetric splitting. The probability of the CN or DNS formation,

$$P_{Z_1,A_1}(E_{\rm c.m.}, J) \sim \exp[-U(R_m, Z_1, A_1, J)/T_{\rm max}(J)], \qquad (4)$$

is calculated statistically by using the stationary solution of the master equation with respect to the charge and mass asymmetries and depends on the potential energy of the CN or DNS configurations and on the thermodynamical temperature. Here, n, p, d, and t evaporation channels are taken into consideration with $U(R_m, Z_1, A_1, J) = 0$. The potential energy

$$U(R_m, Z, A, J) = B_1 + B_2 + V(R_m, Z, A, J) - \left[B_{12} + E^{\rm rot}_{12}(J)\right]$$

of the DNS configuration is calculated with respect to the potential energy $B_{12} + E^{\rm rot}_{12}(J)$ [B_{12} and $E^{\rm rot}_{12}(J)$ are the mass excess and the rotational energy of the CN, respectively] of the rotating CN, R_m is the position of the minimum of the pocket in the nucleus-nucleus interaction potential V, and B_1 and B_2 are the mass excesses of fragments in their ground states.

The probability

$$P^R_{Z_1,A_1}(E_{\rm c.m.}, J) \sim \exp\left[-B^{qf}_R(Z_1, A_1, J)/T_{Z_1,A_1}(J)\right] \qquad (5)$$

of the DNS decay in R coordinates is calculated by using the transition state method. This probability depends on the difference B^{qf}_R (the quasifission barrier) between the potential energies of the DNS configurations at the touching distance and at the Coulomb barrier position.

In Eqs. (4) and (5), $T_{\rm max}(J) = \max\{T_{Z_1,A_1}(J)\}$, where $T_{Z_1,A_1}(J)$ are the temperatures of the CN and all possible DNS. For the emission of particles with $Z_1 < 2$, $T_{Z_1,A_1}(J) = T_{\rm CN}(J)$ is the temperature of the CN and $B^{qf}_R(Z_1, A_1, J)$ is equal to the particle binding energy plus the value of the corresponding Coulomb barrier at $Z_1 \neq 0$. The Fermi-gas model is employed to compute the temperature [20–23].

The neutron-deficient isotopes of nuclei are usually produced in very weak decay channels and their absolute production cross sections are very sensitive to the excitation energy, which is available for light particle or cluster emission. Therefore, we took into account the kinetic energy distributions of emitted light particles (n, p, d, and t) and clusters (^{3}He, ^{4}He, ^{12,14}C, ...) as

$$P(\epsilon, J) = N\epsilon \exp[-\epsilon/T_{Z,A}(J)], \qquad (6)$$

where ϵ is the kinetic energy of light particle or cluster in the center-of-mass system and N is the normalization constant. The actual value of ϵ in each decay event is chosen by the Monte Carlo method.

In the calculations, we use formulas (1) and (3) to treat the sequential statistical decay (the evaporation of light particles and/or the binary decay) of the hot CN. The generation of the whole cascade of decay channels is performed with the Monte Carlo method. We continue to trace the decay processes until all fragments become cold (when the excitation energy of fragments is smaller than the energy threshold of the neutron emission).

III. CALCULATED RESULTS AND DISCUSSIONS

In order to calculate the potential energy in Eq. (4), one can use the experimental [25], if available, or theoretical [16,26–28] values of mass excesses. As follows from Ref. [28], one-proton separation energies $S_{1p} = 0.33, 0.23, 0.76$ MeV, two-proton separation energies $S_{2p} = -1.45, -1.43, -0.3$ MeV, and energies released in α emission $Q_\alpha = 5.08, 4.02, 3.8$ MeV are for ^{108}Xe, ^{112,113}Ba, respectively. So, these nuclei are stable against one-proton emission and unstable against two-proton and alpha emission. To estimate the corresponding half-lives $T_{1/2}$, we can use one of the expressions in Refs. [13,29]. With the expression of Ref. [13] and listed Q_α we find $T_{1/2} \approx 1$ μs, 1 s, and 10 s for alpha emission from ^{108}Xe, ^{112,113}Ba, respectively. The half-lives with respect to two-proton emissions are many orders of magnitude larger. So,

TABLE I. The calculated excitation energy E^*_{CN} [MeV] at $J = 0$ and maximum angular momentum J_{max} of the compound nuclei formed in the indicated reactions at bombarding energies E_{lab} (MeV/nucleon) in the laboratory frame.

E_{lab}	^{58}Ni + ^{58}Ni		^{56}Ni + ^{58}Ni		^{58}Ni + ^{54}Fe		^{56}Ni + ^{54}Fe	
	E^*_{CN}	J_{max}	E^*_{CN}	J_{max}	E^*_{CN}	J_{max}	E^*_{CN}	J_{max}
3.4	32.1	8			38.5	19	35	12
3.6	37.9	29	33.1	22	44	34	40.6	28
3.8	43.7	40	38.8	36	49.6	44	46	39
4.0	49.5	50	44.6	46	55.2	52	51.5	47
4.2	55.3	58	50.2	54	60.8	59	57	54
4.4	61.1	65	56	60	66.4	64	62.5	61
4.6	66.9	71	61.6	67	72	69	68	67
4.8	72.7	76	67.3	72	77.6	75	73.5	72
5.0	78.5	78	73	76	83	75	79	72
5.2	84.3	78	78.7	76	88.4	75	84.5	72
5.4	90.1	78	84.4	76	93.8	75	90	72
5.6	95.9	78	90.1	76	99.2	75	95.5	72
5.8	101.7	78	95.8	76	104.6	75	101	72
6.0	107.5	78	101.5	76	110	75	106.5	72

the main decay mode of neutron-deficient nuclei considered here is α radioactivity.

Because the CN formed in the reactions ^{58,56}Ni + ^{54}Fe and ^{58,56}Ni + ^{58}Ni are very neutron-deficient, the emission of neutrons from the CN is strongly suppressed. The probabilities of very weak decay channels which lead to the formation of isotopes $^{108–110}$Xe and $^{112–114}$Ba are very sensitive to the excitation energy and angular momentum of the system. At angular momenta $J > 60$, the quasifission process from nearly symmetric configurations dominates in these reactions and therefore the evaporation residue cross sections are small. In Table I, one can observe that the maximum angular momenta J_{max} are larger than $J = 60$ at bombarding energies of about (4.2–4.4) MeV/nucleon.

At fixed bombarding energy, the excitation energy of CN decreases with increasing angular momentum (Fig. 1). This effect causes the change of the set of energetically possible decay channels leading to the formation of certain evaporation residues. For example, in the ^{58}Ni + ^{54}Fe reaction at $E_{lab} = 4.2$ MeV/nucleon, the excitation energy changes from $E^*_{CN}(J = 0) \approx 61$ MeV to $E^*_{CN}(J = J_{max}) \approx 30$ MeV.

A. Production of isotopes $^{108–110}$Xe

The complete fusion-evaporation reactions ^{58}Ni + ^{54}Fe $\rightarrow$ $^{108–110}$Xe + (4–2)n and ^{56}Ni + ^{54}Fe $\rightarrow$ ^{108,109}Xe + $1n,2n$ are the most optimal ones for the production of isotopes $^{108–110}$Xe. In the ^{58}Ni + ^{54}Fe reaction, the calculated production cross sections of isotopes ^{109,110}Xe are in a reasonable agreement with the available experimental data [30] (Fig. 2). The maximum cross sections for the production of ^{108}Xe are about 1 nb and 63 nb in the reactions with stable and radioactive Ni beams, respectively. The corresponding optimal incident energies of ^{56,58}Ni are $E_{lab} \approx 4.2$ and 4.6 MeV/nucleon. Note that the prediction within the statistical code HIVAP

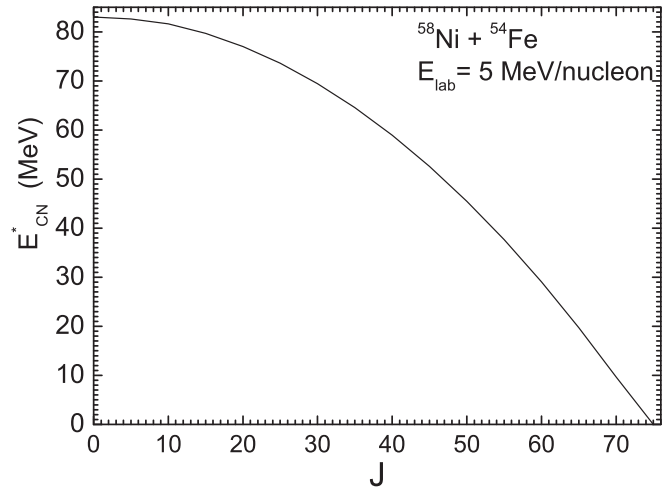

FIG. 1. Dependence of the excitation energy of the CN formed in the ^{58}Ni + ^{54}Fe reaction at 5.0 MeV/nucleon on the angular momentum J.

gives the optimal energy $E_{lab} \approx 4.4$ MeV/nucleon in the ^{54}Fe(^{58}Ni,$4n$)^{108}Xe reaction [30].

The isotopes $^{108–110}$Xe can be also produced in the reactions ^{58,56}Ni + ^{58}Ni via αxn and $2pxn$ evaporation channels. The corresponding excitation functions are presented in Fig. 3. In the ^{58}Ni + ^{58}Ni reaction, the isotopes $^{108–110}$Xe are mostly produced in the αxn ($x = 2–4$) decay channels. The maximum production cross section of the ^{108}Xe isotope is 0.32 nb at $E_{lab} \approx 5.2$ MeV/nucleon. In the reaction with radioactive beam ^{56}Ni, the isotopes ^{108}Xe and ^{110}Xe are produced in the $\alpha 2n$- and $2p2n$-evaporation channels, respectively. For the ^{108}Xe nucleus, the maximum cross section is 23 nb at $E_{lab} \approx$ 4.4 MeV/nucleon. The excitation function for production of isotope ^{109}Xe in the ^{56}Ni + ^{58}Ni reaction has two maxima corresponding to the $\alpha 1n$ and $2p3n$ evaporation channels at 3.8 and 4.8 MeV/nucleon, respectively.

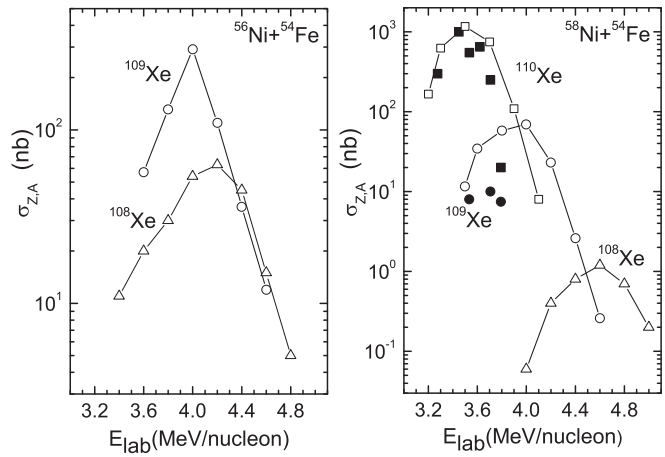

FIG. 2. Calculated excitation functions (open symbols connected by lines) for the production of isotopes $^{108–110}$Xe in the reactions ^{58,56}Ni + ^{54}Fe are compared to the available experimental data (solid symbols) from Ref. [30].

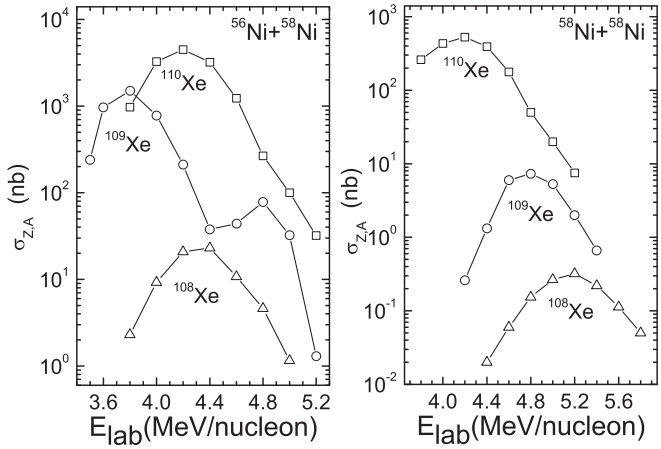

FIG. 3. Calculated excitation functions (symbols connected by lines) for the production of isotopes $^{108–110}$Xe in the reactions ^{58,56}Ni + ^{58}Ni.

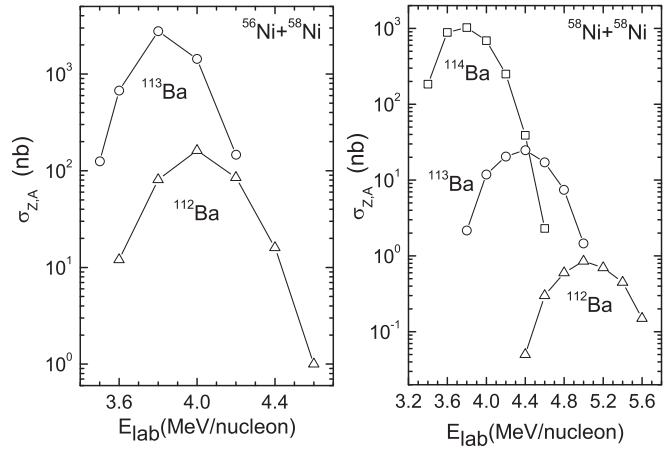

FIG. 4. Calculated excitation functions (symbols connected by lines) for the production of isotopes $^{112–114}$Ba in the reactions ^{58,56}Ni + ^{58}Ni.

B. Production of isotopes $^{112–114}$Ba

The excitation functions for the production of barium isotopes $^{112–114}$Ba in the complete fusion reactions ^{58,56}Ni + ^{58}Ni are depicted in Fig. 4. In Ref. [10], the experimental production cross section of ^{114}Ba in the ^{58}Ni + ^{58}Ni reaction is found to be 200 nb at (3.5–4.2) MeV/nucleon. Our calculations show that the maximum production cross section for ^{114}Ba is about 1 μb at a beam energy 3.8 MeV/nucleon, while at 4.2 MeV/nucleon the cross section falls to 250 nb. One can synthesize ^{112}Ba with production cross sections of 0.85 nb and 160 nb in the reactions ^{58}Ni + ^{58}Ni at 4.9 MeV/nucleon and ^{56}Ni + ^{58}Ni at 4 MeV/nucleon, respectively.

IV. SUMMARY

We applied the DNS model to calculate the excitation functions for the production of neutron-deficient isotopes $^{108–110}$Xe and $^{112–114}$Ba in the fusion-evaporation reactions ^{56,58}Ni + ^{54}Fe and ^{56,58}Ni + ^{58}Ni with stable and radioactive beams. The predicted maximum production cross sections of ^{108}Xe (^{112}Ba) are 63 nb (160 nb) and 1 nb (0.85 nb) in the reactions ^{56}Ni + ^{54}Fe at 4.2 MeV/nucleon (4 MeV/nucleon) and ^{58}Ni + ^{54}Fe at 4.6 MeV/nucleon (4.9 MeV/nucleon), respectively. In the reactions ^{56}Ni(4.4 MeV/nucleon)+^{58}Ni and ^{58}Ni(5.2 MeV/nucleon)+^{58}Ni, the production cross sections of ^{108}Xe are 23 nb and 0.32 nb, respectively. Thus, using the ^{58}Ni + ^{54}Fe reaction with a stable beam, one can study superallowed α-decay chains ^{108}Xe $\rightarrow$ ^{104}Te $\rightarrow$ ^{100}Sn and ^{112}Ba $\rightarrow$ ^{108}Xe $\rightarrow$ ^{104}Te $\rightarrow$ ^{100}Sn and the nuclear properties of the doubly magic nucleus ^{100}Sn with reasonable statistics.

ACKNOWLEDGMENTS

This work was partially supported by RFBR and the IN2P3-JINR Cooperation program.

[1] A. Andreyev *et al.*, Nature (London) **405**, 430 (2000).
[2] E. Roeckl, in *Nuclear Decay Modes*, edited by D. N. Poenaru (IOP, Bristol, 1996), p.237.
[3] H. Schatz, A. Aprahamian, V. Barnard, L. Bildsten, A. Cumming, M. Ouellette, T. Rauscher, F.-K. Thielemann, and M. Wiescher, Phys. Rev. Lett. **86**, 3471 (2001).
[4] R. D. Macfarlane and Antti Siivola, Phys. Rev. Lett. **14**, 114 (1965).
[5] D. Schardt *et al.*, Nucl. Phys. A **368**, 153 (1981).
[6] D. Seweryniak, K. Starosta, C. N. Davids, S. Gros, A. A. Hecht, N. Hoteling, T. L. Khoo, K. Lagergren, G. Lotay, D. Peterson, A. Robinson, C. Vaman, W. B. Walters, P. J. Woods, and S. Zhu, Phys. Rev. C **73**, 061301(R) (2006).
[7] S. N. Liddick, R. Grzywacz, C. Mazzocchi, R. D. Page, K. P. Rykaczewski, J. C. Batchelder, C. R. Bingham, I. G. Darby, G. Drafta, C. Goodin, C. J. Gross, J. H. Hamilton, A. A. Hecht, J. K. Hwang, S. Ilyushkin, D. T. Joss, A. Korgul, W. Krolas, K. Lagergren, K. Li, M. N. Tantawy, J. Thomson, and J. A. Winger, Phys. Rev. Lett. **97**, 082501 (2006).
[8] I. G. Darby, R. K. Grzywacz, J. C. Batchelder, C. R. Bingham, L. Cartegni, C. J. Gross, M. Hjorth-Jensen, D. T. Joss, S. N. Liddick, W. Nazarewicz, S. Padgett, R. D. Page, T. Papenbrock, M. M. Rajabali, J. Rotureau, and K. P. Rykaczewski, Phys. Rev. Lett. **105**, 162502 (2010).
[9] A. Guglielmetti, R. Bonetti, G. Poli, P. B. Price, A. J. Westphal, Z. Janas, H. Keller, R. Kirchner, O. Klepper, A. Piechaczek, E. Roeckl, K. Schmidt, A. Plochocki, J. Szerypo, and B. Blank, Phys. Rev. C **52**, 740 (1995).
[10] Z. Janas *et al.*, Nucl. Phys. A **627**, 119 (1997).
[11] C. Mazzocchi *et al.*, Phys. Lett. B **532**, 29 (2002).
[12] D. N. Poenaru, W. Greiner, and E. Hourani, Phys. Rev. C **51**, 594 (1995).
[13] C. Qi, F. R. Xu, R. J. Liotta, and R. Wyss, Phys. Rev. Lett. **103**, 072501 (2009).

[14] D. N. Poenaru, R. A. Gherghescu, and W. Greiner, Phys. Rev. Lett. **107**, 062503 (2011).
[15] S. N. Kuklin, G. G. Adamian, and N. V. Antonenko, Phys. Rev. C **71**, 014301 (2005).
[16] N. Wang, Z. Liang, M. Liu, and X. Wu, Phys. Rev. C **82**, 044304 (2010).
[17] V. V. Volkov, Izv. AN SSSR Ser. Fiz. **50**, 1879 (1986); G. G. Adamian, A. K. Nasirov, N. V. Antonenko, and R. V. Jolos, Phys. Part. Nuclei **25**, 583 (1994); G. G. Adamian, N. V. Antonenko, and W. Scheid, Nucl. Phys. A **618**, 176 (1997); G. G. Adamian, N. V. Antonenko, W. Scheid, and V. V. Volkov, *ibid.* **627**, 361 (1997); **633**, 409 (1998); G. G. Adamian, N. V. Antonenko, and W. Scheid, Phys. Rev. C **68**, 034601 (2003).
[18] G. G. Adamian, N. V. Antonenko, and W. Scheid, in *Clusters in Nuclei*, Vol. 2, edited by by Christian Beck, Lecture Notes in Physics Vol. 848 (Springer-Verlag, Berlin, 2012), p. 165.
[19] S. A. Kalandarov, G. G. Adamian, N. V. Antonenko, and J. P. Wieleczko, Phys. Rev. C **90**, 024609 (2014).
[20] Sh.A. Kalandarov *et al.*, Phys. Rev. C **84**, 064601 (2011).
[21] S. A. Kalandarov, G. G. Adamian, N. V. Antonenko, and W. Scheid, Phys. Rev. C **83**, 054611 (2011).
[22] S. A. Kalandarov, G. G. Adamian, N. V. Antonenko, W. Scheid, S. Heinz, V. Comas, S. Hofmann, J. Khuyagbaatar, D. Ackermann, J. Heredia, F. P. Heßberger, B. Kindler, B. Lommel, and R. Mann, Phys. Rev. C **84**, 054607 (2011).
[23] G. Ademard, J. P. Wieleczko, J. Gomez del Campo, M. La Commara, E. Bonnet, M. Vigilante, A. Chbihi, J. D. Frankland, E. Rosato, G. Spadaccini, S. A. Kalandarov, C. Beck, S. Barlini, B. Borderie, R. Bougault, R. Dayras, G. De Angelis, J. De Sanctis, V. L. Kravchuk, P. Lautesse, N. Le Neindre, J. Moisan, A. D'Onofrio, M. Parlog, D. Pierroutsakou, M. F. Rivet, M. Romoli, R. Roy, G. G. Adamian, and N. V. Antonenko, Phys. Rev. C **83**, 054619 (2011).
[24] Sh. A. Kalandarov, G. G. Adamian, N. V. Antonenko, and W. Scheid, Phys. Rev. C **82**, 044603 (2010); Sh. A. Kalandarov, G. G. Adamian, and N. V. Antonenko, Phys. Part. Nuclei **43**, 825 (2012).
[25] M. Wang, G. Audi, A. H. Wapstra, F. G. Kondev, M. MacCormick, X. Xu, and B. Pfeiffer, Chin. Phys. C **36**, 1603 (2012).
[26] P. Möller *et al.*, At. Data Nucl. Data Tables **59**, 185 (1995).
[27] M. Liu, N. Wang, Y. Deng, and X. Wu, Phys. Rev. C **84**, 014333 (2011).
[28] N. Wang, M. Liu, X. Wu, and J. Meng, Phys. Lett. B **734**, 215 (2014).
[29] Y. Z. Wang, S. J. Wang, Z. Y. Hou, and J. Z. Gu, Phys. Rev. C **92**, 064301 (2015).
[30] A. Korgul, K. P. Rykaczewski, C. J. Gross, R. Grzywacz, S. N. Liddick, C. Mazzocchi, J. C. Batchelder, C. Bingham, I. Darby, C. Goodin, J. H. Hamilton, J. K. Hwang, S. V. Ilyushkin, W. Królas, and J. A. Winger, Phys. Rev. C **77**, 034301 (2008).